Combined stratigraphic-structural play characterization in hydrocarbon exploration: a case study of Middle Miocene sandstones, Gulf of Suez basin, Egypt

Ahmed. E. Radwan [1,4*], Sébastien Rohais[2], Domenico Chiarella[3]

1 Faculty of Geography and Geology, Institute of Geological Sciences, Jagiellonian University, Gronostajowa 3a; 30-387 Kraków, Poland

2 IFP Energies nouvelles, 1 et 4 avenue de Bois-Préau, 92852 Rueil-Malmaison, France

3 Clastic Sedimentology Investigation (CSI), Department of Earth Sciences, Royal Holloway, University of London, Egham, United Kingdom

4 Exploration Department, Gulf of Suez petroleum company, 2400, Cairo, Egypt

Corresponding author Email: radwanae@yahoo.com

Abstract

As most hydrocarbon discoveries in the Gulf of Suez basin are in structural traps, little research has focused on the evaluation of stratigraphic or combined play in the region. The Badri field represents one of the most prolific oil and gas fields in the Gulf of Suez basin with a large cumulative production from the Miocene Belayim and Kareem Reservoirs. However, Middle Miocene Baba sandstones is still relatively underexplored when compared to other prolific producing reservoir intervals. Recent drilling data from the Badri field has renewed interest in this Member as a reservoir unit due to the lateral facies variations from shale to sandstones recognized in some wells. This study aims to investigate the structural and stratigraphic characterization and hydrocarbon potentiality of Serravalian Baba sandstones. An integrated mineralogical, sedimentological, petrophysical, and reservoir characterization analysis was conducted to obtain and evaluate information about the main reservoir characteristics of Baba sandstones using thin sections, wireline logs (i.e. Resistivity, Density-Neutron, Gamma-ray, and Sonic), and subsurface geologic mapping. Results support that Baba sandstones interval has good

reservoir properties and high potentiality to produce hydrocarbon increasing the reserves in the studied area. Moreover, the entrapment style of Baba sandstones interval is due to the combined effect of stratigraphic and structural components. Accordingly, this study recommends more attention for the stratigraphic and combined stratigraphic-structural traps present along the Gulf of Suez basin.

Keywords: Combined stratigraphic-structural traps, Petrophysics, Petrography, Hydrocarbon, Gulf of Suez, Subsurface analysis, Reservoir characterization.

1.Introduction

Hydrocarbon exploration in the Gulf of Suez basin started more than 100 years ago at Ras Gemsa, with hydrocarbon discovered in the Miocene and Pre-Miocene reservoirs intervals (Fig. 1). Colletta et al. (1998) discussed multiple phases of rifting in the Basin that resulted in a complex tectonostratigraphic evolution and further studies refer to this point (Lyberis,1988; Jarrige, et al., 1990; Patton et al., 1994; Bosworth et al., 1998; Bosworth and McClay, 2001; Lewis et al., 2017). Extensive exploration studies were conducted in the basin to maximize the oil production, which is vital for the Egyptian economy (Elzarka and Moustafa, 1988; Abdine et al., 1992; Khalil and Mesbah, 1998; Dancer et al., 2010; Attia et al., 2015; Mostafa et al., 2015; Abdelghany et al., 2021; Kassem et al.,2021; Radwan et al., 2021). Long exploration history in the Gulf of Suez, resulted in the discovering of more than 80 hydrocarbon fields (Moustafa and Khalil et al., 2020). The rift basin exploration history before twenty century (2000s) was directed to structural highs (i.e. crests of the tilted blocks), which resulted in large reserves that reach up to 10 billion stock barrels of original oil (Youssef, 2011). More than 4 billion barrels are the estimated undiscovered oil resources in the Miocene stratigraphic traps (Meshref et al., 1988; Tewfik et al., 1992; Hassouba et al., 1993, 1994; Dolson and El Gendi et al., 1997; Salama et al., 1994; Youssef, 2011). So recently the exploration strategy in the basin pays more attention to

stratigraphic, structural lows, and sequence stratigraphy application (i.e. Miocene half-grabens or sub-basins) between the high blocks, these type of traps is mostly linked to Miocene sandstones (Young et al., 2000 and 2003; Pivnik et al., 2003; Youssef, 2011; Sarhan, 2020). However, many risks are still exist for exploring Miocene stratigraphic traps, due to the unpredictable lateral distribution and the limited volume of the clastic reservoirs.

The Badri field contains hydrocarbon in the Miocene Belayim and Kareem Reservoirs (EGPC, 1996; Abudeif et al., 2016; Radwan, 2020a-d) The base of the Belayim Formation consists of Baba Member evaporitic sequence. However, some wells show blocky sandstones reported in the literature as Baba sandstones (Abudeif et al., 2018; Attia et al., 2015). Baba sandstones are characterized by high resistivity suggesting good petrophysical characteristics as a potential reservoir in the studied area. However, the facies distribution, hydrocarbon habitat, and trapping mechanism have not been understood and need detailed study.

The main aims of this study are to 1) evaluate the hydrocarbon prospectivity of Baba sandstones through the evaluation of their facies distribution, petrographic, and petrophysical properties, 2) interpret and update the hydrocarbon habitat and petroleum system for the studied unit according to the previous publications and geological based interpretations, 3) enhancing the hydrocarbon recoveries by adding new opportunities in the existing field. The novelty of hydrocarbon prospectivity of Baba sandstones will hopefully provide new insights for exploring the nonstructural plays and focusing on facies or lithology change in the area of Gulf of Suez basin.

2. Geologic setting

The Gulf of Suez basin is a rift basin that contains the major oil-bearing province in Egypt, and that was formed through the separation of the African and Arabian plates during the Late Oligocene - Early Miocene time (Bosworth and McClay, 2001; Abudeif et al., 2016a,b and 2018;

Lashin and Abd El-Aal, 2004; Gawthorpe et al., 2033a,b; Attia et al., 2015; Lewis et al., 2017; Rohais et al, 2016; Radwan et al., 2020a-d; Rohais and Rouby, 2020). The Badri field is located in the southern area of the Gulf of Suez basin and covers an area of about 12 km^2 (Fig. 1) The Badri structure was first drilled in 1966 by a step-out well from the El Morgan Field, which is located immediately to the west of the Badri field across an NNW-striking fault (Radwan et al., 2019a-d; Radwan and Sen, 2020) (Fig. 2). The structure is characterized by a main extensional fault that separates the East Badri and Badri fields with a throw of 460 meters at the top of the Belayim Formation (Radwan, 2014, 2018). In addition, a minor structural element called fault z with a throw of 45 meters at the top of the Belayim Formation is mapped in the northern area of the field (Fig. 3) (Radwan, 2014, 2018; Radwan et al., 2019b, 2020a,c).

3. Lithostratigraphy

The lithostratigraphic succession of the Gulf of Suez basin has been divided into three different stages (Fig.1C): 1) Pre-rift units (pre-Oligocene), 2) Syn-rift units (Oligo-Miocene), and 3) Post-rift units (Quaternary). The syn-rift sediments are characterized by their overall excellent oil potentiality as a source, reservoir, and seal rocks (Richardson et al., 1988; Jackson et al., 2006; Attia et al., 2015; Lewis et al., 2017; Radwan et al., 2019b, c).

The syn-rift Miocene succession is subdivided into the six main formations from base to top: The Nukhul, Rudeis, Kareem the Belayim, South Gharib, and Zeit Formations (EGPC 1964; Fig. 4). The post-Zeit succession attributed to the Plio-Pleistocene is interpreted as post-rift deposits (Fig. 4).

The syn-rift Belayim Formation (Middle Miocene) consists of four Members: Hammam. Faraun (Top), Feiran, Sidri, and Baba (Bottom) (Fig. 5) (Abd-Elshafy and Abu-Ellile 1989; Alsharhan, 2003; Radwan et al., 2019a,b; Nabawy and El Sharawy, 2015; Ali et al., 2016; Nabawy and Barakat, 2017; Radwan, 2020a-d; Radwan et al., 2021). The sandstones recognized

in the Gulf of Suez basin have a good reservoir quality and petroleum accumulation history. The Hammam Faraun Member is the thickest sandstones Member that reaches up to 100 m in the study area and consists of sandstones intercalated with shale and siltstones (Attia et al., 2015; Radwan, 2014,2018). Baba and Feiran Members consist of evaporite deposits, while the Sidri Member is composed of shale with thin sandstones beds intercalated (Fig 5). Baba Member (Serravallian) consists of anhydrite with a thin interbedded clastic marker in the middle part, which allows a subdivision of this Member into three lithologic units. The upper and the lower lithological units are mainly composed of anhydrite in the study area, the middle part is represented by clastic sediments. Each lithological unit is easily laterally correlatable throughout the Badri field. Here, Baba Member varies in thickness from approximately 21 m in the south to almost 91 m in the northern area. In the Badri field, the interbedded clastic unit is less than 15 m thick, and shale represents the main lithology although in some areas wells have penetrated sandstones interval hereafter called Baba sandstones.

4. Material and Methods

The data sets were provided by the Egyptian General Petroleum Corporation (EGPC), through the Gulf of Suez Petroleum Company (GUPCO). Four wells named Badri (A, B, C, and D) represent the core data set in this work. The data consist of formation evaluation logs including Gamma-ray (GR), Density Logs (RHOB), Neutron Logs (NPHI), Compressional Sonic Logs (CODT), formation Resistivity logs (RT), and formation pressure data (MDT). In addition, composite logs, mud logs, and geological reports were used to evaluate Baba clastic interval within the Badri Field as well as to characterize the facies distribution supported by the petrographic analysis. No core data are available for the studied interval, so we depend on the ditch cutting samples. More than 40 ditch samples and 32 thin sections from the four offset wells were used to define the petrographic characteristics of the studied zone. The thin-sections were

studied by using a Nikon polarizing microscope and during this procedure detrital minerals, lithology, grain size, sedimentological features, accessory minerals, visual porosity, and cementation type were determined. The point count method was used for porosity analysis in thin section samples. Sandstones classification was done according to Dott (1964).

Petrophysical investigations used the traditional conventional logs according to the standard procedures available in the literature (Dresser, 1979; Abudeif et al, 2016a and b; Schlumberger, 1986; Darwin, 1987; Alberty, 1992; Atlas, 1995; Attia et al., 2015; Asquith et al., 2004; Abudeif et al., 2018; Schlumberger, 1987; Radwan, 2020c). The petrophysical parameters have been analyzed using the Techlog© software. The shale volume has been determined using the density neutron method due to the presence of feldspars in the studied sandstones (Asquith, 1990) (Eq.1) (Table 1). The density-neutron method was used to calculate the total porosity (Serra, 1983) (Eq.2) (Table 1). Effective porosity was calculated using the volume of clay and neutron porosity of pure shale (Hill et al., 1979; Clavier et al., 1984; Juhasz, 1986; Schlumberger, 1989; Alberty, 1992) (Eq.3) (Table 1). Water saturation was calculated using the Archie equation (Archie, 1942) (Eq.4) (Table 1). Permeability was estimated using Wyllie and Rose Approach (Wylie and Rose, 1950) (Eq.5 and 6) (Table 1). Hydrocarbon volume calculation was done using the standard volumetric method for hydrocarbon calculations (Bishop et al., 1983; Shepherd, 2009; Attia et al., 2015) (Eq.7 and 8) (Table 1).

4. Results

4.1. Baba clastics marker distribution

All drilled wells in the study area confirmed that the stratigraphic section of Baba Member consists mainly of two anhydrite units separated by a clastic marker interval (Figs 1 and 5). Anhydrite is characterized by white and tannish white color, and moderately hard. The thickness of the clastic interval ranges from 5 to 15 m, and the facies consists mainly of shale. Towards the

north of the field, shales laterally grade into blocky sandstones facies (Fig. 5). The blocky sandstones facies has a thickness ranging between 7 to 12 m (Fig. 5). The lateral evolution of Baba sandstones shows that the sandstones decreases in thickness from the east (wells C and D) to the west (wells A and B) (Table. 2). The geographic distribution of Baba sandstones and wells indicate that they encompass a faulted area (fault z), where two wells were drilled in the hanging block (wells C and D) and the other two wells (A and B) in the down-faulted block (Figs. 3 and 6).

Baba deposits (B4 in Rohais et al., 2016) recorded the first disconnection of the entire Gulf of Suez basin rift from the Mediterranean Sea during its rifting stage. Halite deposits were preserved in fault-controlled depocenters (Fig. 7). Sediment supplies along the rift shoulders were very low as suggested by the very small isolated and fan-shaped siliciclastic bodies developed along the Morgan accommodation zone (Fig. 7B). Baba sandstones in the Badri field was probably fed from the El Qaa plain fan bodies, with more sand content to the north, progressively inter-fingering with shale to the south and southwest.

4.2. Petrographic characterization.

Shale is the dominant lithology in the clastics marker of Baba Member. The shale is characterized by different colors including dark grey, light gray, brownish grey, greenish grey, and yellowish grey. The shale firmness is ranging from soft to moderate. The shale reaction with the hydrochloric acid showed slightly calcareous content. Pyrite represents the main accessory mineral. The description of Baba sandstones is mainly based on the thirty-two thin section samples from the studied wells. The average grain-size ranges from coarse to medium-grained sand with rarely fine-grained sand and pebble-sized grains locally present (Table.3). According to the ternary plot, Baba sandstones can be classified as Arkose (*Q70 F27 L3*) (Fig. 8).

4.2.1. Constituent grains

Baba sandstones consist of four components including quartz, feldspars, lithic fragments, and accessory minerals. The quartz grains of Baba sandstones are dominated by both monocrystalline and polycrystalline quartz ranging from 65% to 74% of the total volume (Table 3). The quartz grains range from sub-rounded to sub-angular in most samples (Table 3). The feldspars component is dominated by plagioclase feldspars while some samples have a significant amount of microcline. The feldspars content ranges from 31% to 24% of the total rock. Some feldspars grains show dissolution and alteration. Lithic fragments and accessory minerals represent a minor component of the total rock volume (~ 3%). The accessory minerals include pyrite as the dominant mineral. Authigenic quartz overgrowths were also observed in some samples. Micas (e.g. biotite, chlorite, and muscovite) are rarely present (Fig. 9 & 10).

4.2.2. Cement and Matrix

The quartz and anhydrite cement are the dominant cementation process affecting Baba sandstones. The silica cement is dominant in most samples while the anhydrite cement is increasing in the up-section. Baba sandstones matrix contains silt-sized grains of quartz and clays (Table 3) (Fig. 9 & 10). In addition, amorphous organic materials are observed in most samples.

4.2.3. Texture or Fabric

The investigated samples of Baba sandstones are dominantly by sub-rounded grains, although sub-angular grains are locally recognized with angularity increasing toward the up-section. The average grain size in the investigated samples are variables from fine-grained sand (160 microns) to gravel sizes (Table 3). Sorting is characterized by variable degrees including moderately, well and poor sorting. The moderately sorted texture is dominant in most samples. Well sorted grains are dominant in the middle part of Baba sandstones.

4.2.4. Porosity

The estimated porosity in thin sections images by point count method is (10-15%) along with Baba sandstones interval (Table 3). The porosity in Baba sandstones is characterized by both

primary and secondary porosity in most samples. The primary porosity is dominant in most samples representing more than 90% of the total porosity. The secondary porosity represents no more than 8 % of the total porosity.

The anhydrite of Baba Member indicates a lagoonal and restricted depositional environment, while the sandstones and shales within Baba Member indicate shallow marine environment (Salah and Alsharhan, 1997; Radwan, 2014; Tawadros, 2012: Rohais et al., 2016; Nabawy and Barakat, 2017; Radwan, 2018; Radwan, 2020a). However, the absence of cores in the studied reservoir, and the unobvious log signatures doesn't allow for taking a step further on defining more facies analysis studies.

4.3. Petrophysical evaluation

Based on the petrophysical evaluations of Baba clastics sandstones reservoir in the investigated Badri (A, B, C, and D) wells, the shale volume (Vsh) analysis shows a low shale content with an average ranging from 9 % to 13%, while the maximum estimated value is 18% (Table 2). In general, the higher values of the gamma-ray log in the blocky sandstones unit are due to the presence of feldspars. The effective porosity (Øeff) shows good porosity with average values ranging from 11% to 17%, and a maximum value of 23%. The higher effective porosity is in the two up-dip wells and the relatively lower porosities occur in the down-dip wells. The water saturation (Sw) analysis shows a reverse trend compared to that of the effective porosity. The water saturation ranges from 12% to 21%, with maximum values up to 21%. The higher water saturation is observed in the down-dip wells and the lower water saturation is in the up-dip wells. The hydrocarbon saturation (Shr) analysis shows high saturation values. The higher hydrocarbon saturation is in the up-dip wells, with the average hydrocarbon saturation was ranged from 79% to 88% (Table. 2). The estimated permeability analysis shows average values ranging from 180 to 220 mD, with a maximum of 400 mD. Fluid type evaluation indicated the presence of oil in BDR (A and B) wells, and gas cap in BDR (C and D) wells (Fig. 11).

4.4. Hydrocarbon volume

The last inferred petrophysical parameters have been used to calculate the estimated hydrocarbon on the studied Member. According to the standard oil industry equations (Eq. 7 and 8) in (Table 1), the (STOOIP) in the studied Member is approximately 1,100,000 Stock tank barrels as P50. In addition, small estimated quantities of gas reach up to 1481 (MM SCF) as P50.

5. Interpretation and synthesis

The primary reservoirs of the Badri Field have been deposited during Middle Miocene just after the rift-climax phase. Rifting formed half-grabens structures that allow the deposition of variable clastic and evaporitic sequence in the Belayim Formation (Fig. 1) (Evans, 1988, 1990; Gawthorpe et al., 1990; Abd El Gawad, 2007; Muravchik et al., 2016; Rohais et al., 2016). In the late middle Miocene thick evaporites, shales were deposited over Middle Miocene sediments forming South Gharib and Zeit Formations, which act as primary seal rocks in the Gulf of Suez basin (A-Rehim et al., 1994; Attia et al., 2015). The studied Baba Member is the basal Member of Belayim Formation and consists of anhydrite, and sediment influxes has been forms clastics marker in between the anhydrite layers along the studied field. The shaly facies pass laterally to sandstones in the northern part of the field. The lateral correlation of this blocky sandstones facies indicated that in the different areas they have the same electrical log response (Fig 6). The existence of these facies in four adjacent wells with the same log characteristics supporting the idea that these sandy facies are laterally continuous. Paleo-geographic reconstructions (Fig. 7) suggest that these sandstones were part of a large fan-shaped siliciclastic body extended across EL Morgan Accommodation Zone and supplied from the El Qaa Plain area (Eastern border of the rift). Another fan-shaped siliciclastic body was also developed is a similar pattern in the western part of the Morgan Accommodation Zone (Fig. 7B).

5.1. Sedimentological interpretations

Porosity investigations of the arkosic sandstones of Baba Member showed predominantly intergranular porosity, as indicated by the thin section photomicrographs (Fig. 9 & 10). In addition, secondary porosity has been recorded in the thin section samples, which may be resulted from the dissolution of feldspar grains. The petrographic analysis points out that Baba clastic sandstones marker unit in Badri (A, B, C, and D) wells is characterized by a wide range of grain-size, porosity, and sorting. Sorting ranges from good to moderate. The observed organic material filling pore space inter grains which may indicate oil pathways or oil-bearing sandstones. The good reservoir quality of Baba sandstones was suggested to be the result of the presence of secondary dissolution pores interconnected with the primary intergranular network. Moreover, the clay minerals, cementation, and compaction were identified as the main porosity-reducing agents. Polycrystalline and monocrystalline quartz grains are usually mechanically stable during weathering and transportation. Consequently, the preservation and the abundance of angular to sub-rounded polycrystalline and monocrystalline quartz grains suggest that sediments pertaining to Baba sandstones experienced short transport. The study of the detrital grains of Baba reservoir indicates that Baba clastics marker reservoir (Serravallian) was driven mainly from nearby exposures of Red Sea Hills. In addition, the presence of polycrystalline quartz suggests igneous source rocks or metamorphic rocks, particularly (gneisses) (El-Ashry, 1972; Salah and Alsharhan, 1997; Attia et al., 2015).

5.2. Petrophysical interpretations

Baba reservoir shows high gamma-ray, low-density readings, relatively porous zone, and high resistivity values (Fig. 6 & 11). It should be noted that the high gamma-ray of Baba sandstones is related to the K-feldspars content within the reservoir, which increases the gamma-ray response. The result of the well log analysis showed that the average effective porosity ranges between 12 and 20% with a significant increase towards the BDR (C and D) wells. Hydrocarbon saturation

ranging from 79% to 88% and increases towards the BDR (C and D) wells. Low shale volume has been estimated to range from 9% as the lowest up to 13% as the maximum and this amount decreases towards the BDR (C and D) wells. According to the well log analysis, it is inferred that the derived petrophysical parameters exhibited good porosity, low clay content, and high hydrocarbon saturation, which indicates that Baba sandstones facies are excellent sandstones unit or reservoir. The petrophysical investigation inferred that the Net Pay to Gross Ratio (NGR) values are equal to 1, which means that net pay is equal to Gross thickness. These sandy facies characteristics have very high potentiality as a hydrocarbon-bearing reservoir within Baba Member.

5.3. Hydrocarbon habitat and petroleum geology

The very high potentiality of the Gulf of Suez basin is related to the fact that the rifting tends to produce both open marine and restricted settings favorable to a source rock accumulation, in addition, the relatively high geothermal gradient (Khalil and Meshref, 1988; Khalil and McClay, 1998; Dolson, et.al, 2001; Alsharhan, 2003; Lewis et al., 2016; El Nady and Mohamed, 2016). The hydrocarbon potential of the exanimated area is proved by the successful wells producing from Middle Miocene reservoirs.

The principal source rocks in the Badri field are the Upper Cretaceous Brown Limestone (Senonian) and the Eocene Thebes Formation (EGPC, 1996). These limestones were deposited under a marine environment with anoxic conditions. Limestone facies contain abundant algal and amorphous kerogen of Types II and II/I, and organic richness of 8 wt.% (Table 4) and (Fig. 13) (Chowdhary and Taha, 1987; Lelek et al., 1992; Hughes et al., 1992; EGPC, 1996; Salah and Alsharhan, 1997). These source rocks are mature and have been generating oil since the latest Miocene to Pliocene times in adjacent deep areas.

The seal rocks in Badri Field consists of evaporites and shales Miocene in age (Chowdhary and Taha, 1987, EGPC, 1996) (Fig. 12 & 13). In the studied area, the upper and lower anhydrite units act as top seal, and the surrounded shale of Baba sandstones facies act as lateral seal. In addition, the structural setting of the field juxtaposed the sandstones facies against the evaporitic seal in the eastern side of the field (Fig. 2 & 12). While Baba shale acts as a lateral seal in the western side of the area (Fig. 12). Oil migrated along the bounding faults, formed after the Mid-Rudeis tectonic event in the late Lower Miocene (EGPC, 1996). Hydrocarbon entrapment seems to have a combined stratigraphic and structural nature. Hence, the studied Baba Member is located between the two principal reservoirs, meaning that the same source rock, migration paths charge the porous zone according to the entrapment and effective seals. The stratigraphic component in Baba sandstones consists of facies change from shale to sandstones. Sediment influx is the key factor that controls the facies change from shale to sandstones in this shallow marine to lagoons deposits. The structural component represents the NW to SE trending anticline with closure of more than 130 meters at the top of Belayim Horizon. To the east, NW to SE trending normal fault bounds the reservoir from the east side with more than one four hundred and fifty meters of throw at the top of Belayim. To the west, the Badri Field is bounded and separated from the North El Morgan Field by NW to SE trending normal fault, dipping NE. This fault juxtaposes the Badri Belayim section against the productive Kareem section in the adjacent El Morgan Field (EGPC, 1996; Radwan et al., 2019a, 2020a) (Fig. 2 & 12). Smaller NW to SE trending normal fault with thirty-meter vertical displacement has been detected in the NE portion of Badri Field, which affected the studied Baba sandstones (Fig. 3 & 12). A summary chart of hydrocarbon habitat (source rocks, seals, and reservoirs) and their distribution relative to the formations and geologic ages is shown in (Fig. 13). Accordingly, the trap style for the investigated sandstones facies consists of combined stratigraphic and structural components.

5.4. Implications for exploring combined traps in the basin

Exploring stratigraphic and combination traps have had less priority from the beginning of the oil and gas revolution until the twenty century. Stratigraphic traps have historically been viewed as a high risk (Stirling et al., 2017). Non-structural traps were comprising lower than 20% volume of the structural traps worldwide (Dolson et al., 2017). Acquiring 3D seismic imaging at the beginning of twenty century has led to an enhancement of the seismic resolution, and develop hydrocarbon system modeling. Moreover, the application of sequence stratigraphy concept in hydrocarbon exploration contributed to look over structural traps. Accordingly, many large stratigraphic or combined prospects have been explored (e.g. offshore Ghana and Mozambique and the Utsira High in the North Sea). The economic success of these traps has spotted the light on these under-explored remains globally (e.g. tight gas in the China Ordos Basin) (Attia et al., 2015; Dolson et al., 2017; Arab et al., 2016; Nguyen et al., 2019; Hall et al., 2019; Sladen and Chiarella, 2020).

Multiple chances for exploring new resources along unconformity surfaces, pinch-out, and carbonate reef could then represent a major opportunity for the Gulf of Suez basin as well. To enhance the exploration effectiveness of stratigraphic and combined traps, companies should increase the use of seismo-stratigraphy, biostratigraphy, and lithostratigraphy approaches along with the sequence stratigraphy one (Dolson, 1999; Young et al., 2000 and 2003). In this context, analysis of lateral seals needs large consideration while prospecting risk evaluations using the same approach. In the present study, the paleogeographic maps during the deposition of the Baba Mb. give insight on the potential pinch-out and stratigraphic traps surrounding the known reservoir area. This requires a structural restoration as well as putting the area of interest into perspective in a larger basin-scale context.

In the last decades, non-structural traps have been discovered accidentally in the Gulf of Suez basin (Alsharhan, 2003). Most of these fields are only small accumulations located in flank positions to the tilted block crests (Dolson et al., 2017). However, although studies within the last

decades have provided a good understanding of the petroleum system of the area, main exploration resources are still focused on the same traditional structural traps, and not exploring the synclinal basins. The study case presented in this work can then highlight the potentiality for further development of near-field exploration in the Gulf of Suez basin and surrounded areas.

6. Conclusions

Our multidisciplinary analysis allows us to evaluate the reservoir architecture and the structural and stratigraphic characterization of the Middle Miocene Baba sandstones. The main conclusions of our study can be summarized as follows:

- Our sedimentological analysis revealed that there is a correlatable clastic marker within the evaporitic Baba Member, and this unit consists of shale laterally passing into blocky sandstones in the northern part of the Badri Field. The stratigraphic analysis suggests that the Baba sandstones decreases in thickness and pinch-out towards the west.
- The petrographic and petrophysical characteristics of the Middle Miocene sandstones suggests that this unit has a pretty consistent mineralogical composition and it pertains to the same depositional environment throughout the area. Moreveor, the reservoir characteristics suggest that this interval represents a potential reservoir.
- Integration of structural and stratigraphic analysis, as well as characterization of the petroleum elements of the Middle Miocene Baba sandstones suggests the presence of a unique combined stratigraphic-structural trapping mechanism.
- The result of this study could open up a new direction for the petroleum exploration of potential combined traps in the Gulf of Suez basin. In addition, the lateral facies variability recognized along syn-rift sediments of the Gulf of Suez basin represents an

interesting aspect that should be further investigated since it might open a new potential target (i.e. stratigraphic traps) for hydrocarbon exploration and development in the basin.

- The combined stratigraphic-structural play characterization presented in this work highlights the hydrocarbon potentiality for further development of near-field exploration in the Gulf of Suez basin and surrounded areas. Accordingly, further studies are needed to extend the knowledge in the adjacent fields, and additional targets such as the Baba and Sidri sandstones must be assessed in further exploration plans.

Acknowledgments

The author expresses his thanks to the Egyptian General Petroleum Corporation and Gulf of Suez Petroleum Company GUPCO authorities for their permissions to carry out this study and providing data. Ahmed E. Radwan expresses his deepest thanks to the Narodowa Agencja Wymiany Akademickiej (NAWA) under Project PPN/ULM/2019/1/00305/U/00001 for supporting during this research time as well as deep thanks to Prof. Alfred Uchman for his continuous support during the research period.

References

Abd-Elgawad, E. A. 2007. The Use of Well Logs to Determine the Reservoir Characteristics of Miocene Rocks at The Bahar Northeast Field, Gulf of Suez, Egypt. Journal of Petroleum Geology, 30(2), 175–188. doi:10.1111/j.1747-5457.2007.00175.x

Abdelghany, W. K., Radwan, A.E., Elkhawaga, M. A., Wood, D., Sen, S., Kassem, A. A. 2021. Geomechanical Modeling Using the Depth-of-Damage Approach to Achieve Successful Underbalanced Drilling in the Gulf of Suez Rift Basin. Journal of Petroleum Science and Engineering. https://doi.org/10.1016/j.petrol.2020.108311

Abd-Elshafy, E., Abu-Ellile, M. M. 1989. Stratigraphy and correlation of Belayim Cenomanian, Gulf of Suez, Egypt. Journal of African Earth Sciences (and the Middle East), 9(1), 77–85. doi:10.1016/0899-5362(89)90010-9

Abdine, S., Homossani, A., Lelek, J. 1992. October Field the latest giant under development in the Gulf of Suez, Egypt. In International conference on geology of the Arab World (pp. 61-86).

Abudeif, A. M., Attia, M. M., Radwan, A. E. 2016a. Petrophysical and petrographic evaluation of Sidri Member of Belayim Formation, Badri field, Gulf of Suez, Egypt. Journal of African Earth Sciences, 115, 108–120. doi:10.1016/j.jafrearsci.2015.11.028

Abudeif, A. M., Attia, M. M., Radwan, A. E. 2016b. New simulation technique to estimate the hydrocarbon type for the two untested members of Belayim Formation in the absence of pressure data, Badri Field, Gulf of Suez, Egypt. Arabian Journal of Geosciences, 9(3). doi:10.1007/s12517-015-2082-2

Abudeif, A. M., Attia, M. M., Al-Khashab, H. M., Radwan, A. E. 2018. Hydrocarbon type detection using the synthetic logs: A case study, Baba member, Gulf of Suez, Egypt. Journal of African Earth Sciences, 144, 176–182. doi:10.1016/j.jafrearsci.2018.04.017

Alberty, M. 1992. Standard interpretation: Part 4. wireline methods.

Alsharhan, Salah 1994. Geology and hydrocarbon habitat in a rift setting: southern Gulf of Suez, Egypt vol.42. P312-331.

Alsharhan, A. S. 2003. Petroleum geology and potential hydrocarbon plays in the Gulf of Suez rift basin, Egypt. AAPG bulletin, 87(1), 143-180.

Ali, E. K. A., Elrazik, E. A., Azam, S. S., Hassan, S. A. 2016. Integrated petrophysical and lithofacies studies of lower-middle Miocene reservoirs in Belayim marine oil field, Gulf of Suez, Egypt. Journal of African Earth Sciences, 117, 331–344. doi:10.1016/j.jafrearsci.2016.02.007

A-Rehim, E., Hughes, S., Ahmed, H., Steer, B., 1994. The multi-discipline field study approach - Badri Field case study: Proceedings 12th Exploration & Production Conference, Cairo: EGPC, Production v. 2, p. 297-313

Archie, G. E. 1942. The electrical resistivity log as an aid in determining some reservoir characteristics. Transactions of the AIME, 146(01), 54-62

Arab, M., Belhai, D., Granjeon, D., Roure, F., Arbeaumont, A., R. Bracene, A. Lassal, C. Sulzer, Deverchere, J. 2016. Coupling stratigraphic and petroleum system modeling tools in complex tectonic domains: case study in the North Algerian Offshore. Arabian Journal of Geosciences, 9(4). doi:10.1007/s12517-015-2296-3

Asquith, G., Krygowski, D., Henderson, S., Hurley, N. 2004. Log Interpretation. Basic Well Log Analysis. doi:10.1306/mth16823c7

Asquith, G. B., 1990. Log Evaluation of Shaly Sandstones: A Practical Guide. Available at: http://dx.doi.org/10.1306/99a4d061-3318-11d7-8649000102c1865d.

Atlas, W. 1995. Introduction to wireline log analysis. Western Atlas International Inc., Houston, Texas.

Attia, M. M., Abudeif, A. M., Radwan, A. E. 2015. Petrophysical analysis and hydrocarbon potentialities of the untested Middle Miocene Sidri and Baba sandstone of Belayim Formation, Badri field, Gulf of Suez, Egypt. Journal of African Earth Sciences, 109, 120–130. doi:10.1016/j.jafrearsci.2015.05.020

Barakat, A. O., Mostafa, A., El-Gayar, M. S., Rullkötter, J. 1997. Source-dependent biomarker properties of five crude oils from the Gulf of Suez, Egypt. Organic geochemistry, 26(7-8), 441-450.

Bishop, R. S., Gehman, H. M., Young, A. 1983. Concepts for estimating hydrocarbon accumulation and dispersion. AAPG Bulletin, 67(3), 337-348.

Bosworth, W., Crevello, P., Winn, R. D., Steinmetz, J. 1998. Structure, sedimentation, and basin dynamics during rifting of the Gulf of Suez and north-western Red Sea. In Sedimentation and Tectonics in Rift Basins Red Sea:-Gulf of Aden (pp. 77-96). Springer, Dordrecht.

Bosworth W., McClay K. 2001. Structural and stratigraphic evolution of the Gulf of Suez rift, Egypt: a synthesis. Paris Museum National d'Histoire naturelle de Paris, Memoirs. p. 567–606.

Chowdhary, L. R., Taha, S. 1987. Geology and habitat of oil in Ras Budran field, Gulf of Suez, Egypt. AAPG Bulletin, 71(10), 1274-1293.

Clavier, C., Coates, G., Dumanoir, J. 1984. Theoretical and experimental bases for the dual-water model for interpretation of shaly sands. Society of Petroleum Engineers Journal, 24(02), 153-168.

Colletta, B., Quellec, P., Letouzey, J., Moretti, I. 1988. Longitudinal evolution of the Suez rift structure (Egypt). Tectonophysics, 153(1-4), 221–233. doi:10.1016/0040-1951(88)90017-0.

Dancer, P. N., Collins, J., Beckly, A., Johnson, K., Campbell, G., Mumaw, G., Hepworth, B. 2010. Exploring subtle exploration plays in the Gulf of Suez. In Geological Society, London, Petroleum Geology Conference series (Vol. 7, No. 1, pp. 771-781). Geological Society of London.

Darwin.V.E., 1987. "Well Logging for Earth Scientists", Elsevier Science Publishing Co., New York. Pp 401-447.

Darwish, M., El-Araby, A. M., Philobbos, E. R., Purser, B. H. 1993. Petrography and diagenetic aspects of some siliciclastic hydrocarbon reservoirs in relation to the rifting of the Gulf of Suez. Geodynamics and Sedimentation of the Red Sea–Gulf of Aden Rift System. Geological Society of Egypt, Special Publication, 1, 155-187

Dolson, J. C., El Gendi, M.O. 1997. Rift Basin Sequence Stratigraphy Models: Parts A and B, Gulf of Suez Miocene Syn-Rift Deposits: ABSTRACTS. AAPG Bulletin, 81. doi:10.1306/3b05cd48-172a-11d7-8645000102c1865d

Dolson, Shann, Matbouly, Harwood, Rashed, Hammouda, 2001. The Petroleum Potential of Egypt, AAPG Memoir, 74, 453 – 482.

Dolson, J., He, Z., Horn, B. W. 2017. Advances and perspectives on stratigraphic trap exploration-making the subtle trap obvious. In AAPG 2017 Middle East region geosciences technology workshop, stratigraphic traps of the Middle East, Muscat, Oman.

Dolson, J. C., Bahorich, M. S., Tobin, R. C., Beaumont, E. A., Terlikoski, L. J., Hendricks, M. L., Foster, N. H. 1999. Exploring for stratigraphic traps. *Exploring for oil and gas traps:* AAPG Treatise of Petroleum Geology, Handbook of Petroleum Geology, 21-1.

Dresser, A. 1979. Log interpretation charts. Houston, Dresser Industries Inc.

Dott, J., 1964. Wacke, Graywacke and Matrix--What Approach to Immature Sandstones Classification?. Journal of Sedimentary Research, 34(3).

EGPC, 1996. Gulf of Suez oil fields (a comprehensive overview): Egyptian General Petroleum Corporation, Cairo, 736pp

El-Ashry, M. T. 1972. Source and dispersal of reservoir sands in El Morgan field, Gulf of Suez, Egypt. Sedimentary Geology, 8(4), 317-325

El Nady, M. M., Mohamed, N. S. 2016. Source rock evaluation for hydrocarbon generation in Halal oilfield, southern Gulf of Suez, Egypt. Egyptian Journal of Petroleum, 25(3), 383-389

Elzarka, M. H., Mostafa, A. R. 1988. Oil prospects of the Gulf of Suez, Egypt—a case study. Organic geochemistry, 12(2), 109-121.

Evans, A. L. 1988. Neogene tectonic and stratigraphic events in the Gulf of Suez rift area, Egypt. Tectonophysics, 153(1-4), 235-247

Evans, A. L. 1990. Miocene sandstones provenance relations in the Gulf of Suez: insights into synrift unroofing and uplift history. AAPG bulletin, 74(9), 1386-1400

Gawthorpe, R. L., Hurst, J. M., Sladen, C. P. 1990. Evolution of Miocene footwall-derived coarse-grained deltas, Gulf of Suez, Egypt: implications for exploration. AAPG bulletin, 74(7), 1077-1086

Gawthorpe, R. L., Jackson, C. A.-L., Young, M. J., Sharp, I. R., Moustafa, A. R., Leppard, C. W. 2003a. Erratum to: Normal fault growth, displacement localisation and the evolution of normal fault populations: the Hamman Faraun fault block, Suez Rift, Egypt. Journal of Structural Geology, 25(8), 1347–1348. doi:10.1016/s0191-8141(03)00059-2

Gawthorpe, R. L., Jackson, C. A.-L., Young, M. J., Sharp, I. R., Moustafa, A. R., Leppard, C. W. 2003b. Normal fault growth, displacement localisation and the evolution of normal fault populations: the Hammam Faraun fault block, Suez rift, Egypt. Journal of Structural Geology, 25(6), 883–895. doi:10.1016/s0191-8141(02)00088-3

Gradstein F.M., Ogg J.G., Schmitz M.D., Ogg G.M. 2012. The Geologic Time Scale. Elsevier doi:10.1016/B978-0-444-59425-9.10003-4

Hall, L. S., Palu, T. J., Murray, A. P., Boreham, C. J., Edwards, D. S., Hill, A. J., Troup, A. 2019. Hydrocarbon prospectivity of the Cooper Basin, Australia. AAPG Bulletin, 103(1), 31-63

Hammouda, H. 1992. Rift tectonics in the southern Gulf of Suez; gravity and magnetic contribution: 11th Egyptian General Petroleum Corporation Exploration Seminar

Haq B.U., and Al-Qahtani A.M. 2005. Phanerozoic cycles of sea-level change on the Arabian Platform: GeoArabia, v. 10/2, p. 127-160.

Hardenbol J, Thierry J, Farley MB, Jacquin T, de Graciansky PC, Vail P., 1998. Mesozoic and Cenozoic sequence chronostratigraphic framework of European basins, in P.C. Graciansky, et al. (eds) Mesozoic and Cenozoic Sequence Stratigraphy of European Basins: SEPM Special Publication 60, p. 3-13, charts 1-8.

Hassouba, M., El-Shafy, A. A., Shafy, S., Saber, 1993. Application of paleobathymetric analysis in oil exploration of the Miocene sequence in the central Gulf of Suez, Egypt. In International conference on geoscientific research in Northeast Africa (pp. 277-283).

Hewlett, J. S., Jordan, D. W. 1993. Stratigraphic and Combination Traps Within a Seismic Sequence Framework, Miocene Stevens urbidites, Bakersfield Arch, California: Chapter 6: Recent Applications of Siliciclastic Sequence Stratigraphy

Hill, H. J., Klein, G. E., Shirley, O. J., Thomas, E. C., Waxman, W. H. 1979. Bound water in shaly sands-its relation to Q and other formation properties. The log analyst, 20(03)

Hughes, G. W., Abdine, S., Girgis, M. H. 1992. Miocene biofacies development and geological history of the Gulf of Suez, Egypt. Marine and petroleum geology, 9(1), 2-28

Jackson, C. A. L., Gawthorpe, R. L., Sharp, I. R. 2006. Style and sequence of deformation during extensional fault-propagation folding: examples from the Hammam Faraun and El-Qaa fault blocks, Suez Rift, Egypt. Journal of Structural Geology, 28(3), 519-535

Jarrige, J. J., Ott d., P., Burollet, P. F., Montenat, C., Prat, P., Richert, J. P., Thiriet, J. P. 1990. The multistage tectonic evolution of the Gulf of Suez and northern Red Sea continental rift from field observations. Tectonics, 9(3), 441-465.

Juhasz, I. 1986. Assessment of the distribution of shale, porosity and hydrocarbon saturation in shaly sands. In European Formation Evaluation symposium. 10.

Kassem, A. A., Hussein, W. S., Radwan, A. E., Anani, N., Abioui, M., Jain, S., & Shehata, A. A. 2021. Petrographic and Diagenetic Study of Siliciclastic Jurassic Sediments from the Northeastern Margin of Africa: Implication for Reservoir Quality. *Journal of Petroleum Science and Engineering*, 108340. https://doi.org/10.1016/j.petrol.2020.108340

Khalil, M., 1993. Structural Evolution of the B"Trend and its Significance for Hydrocarbon Exploration in Offshore Gulf of Suez, Egypt." AAPG Bulletin, 77. doi:10.1306/bdff81d2-1718-11d7-8645000102c1865

Khalil, B., Meshref, W. 1988. Hydrocarbon occurrences and structural style of the southern Suez rift basin: Egyptian General Petroleum Corp. In Ninth Exploration and Production Conference

Khalil, S., McClay, K., 1998. Structural architecture of the eastern margin of the Gulf of Suez: field studies and analogue modelling results, Proceedings 14th Exploration & Production Conference, Cairo: EGPC, Production v. 1, p. 210-211

Lashin, A., Abd El-Aal, M., 2004. Seismic data analysis to detect the depositional process environments and structural framework of the east central part of Gharib Province, Gulf of Suez-Egypt. Annals of the Egyptian Geological Survey, 27: 523-550

Lelek, J. J., Shepherd, D. B., Stone, D. M., Abdine, A. S.,1992. October Field: The Latest Giant under Development in Egypt's Gulf of Suez: Chapter 15.

Lewis, M. M., Jackson, C. A. L., Gawthorpe, R. L. 2017. Tectono-sedimentary development of early syn-rift deposits: The Abura Graben, Suez Rift, Egypt. Basin Research, 29, 327-351

Lindquist, S. J. 1998. The Red Sea Basin Province: Sudr-Nubia (!) and Maqna (!) Petroleum Systems. DIANE Publishing.

Lyberis, N. 1988. Tectonic evolution of the Gulf of Suez and the Gulf of Aqaba. Tectonophysics, 153(1-4), 209-220

Meshref, W. M., Abu Karamat, M. S., Gindi, M. 1988. Exploration concepts for oil in the Gulf of Suez. In 9th Petroleum Exploration and Production Conference, Cairo (pp. 1-24)

Mostafa, A., Sehim, A., Yousef, M. 2015. Unlocking subtle hydrocarbon plays through 3D seismic and well control: A case study from West Gebel El Zeit district, southwest Gulf of

Suez, Egypt. In Offshore Mediterranean Conference and Exhibition. Offshore Mediterranean Conference.

Moustafa, A. R. 1993. Structural characteristics and tectonic evolution of the east-margin blocks of the Suez rift. Tectonophysics, 223(3-4), 381-399

Moustafa, A. R., Khalil, S. M. 2019. Structural Setting and Tectonic Evolution of the Gulf of Suez, NW Red Sea and Gulf of Aqaba Rift Systems. Regional Geology Reviews, 295–342. doi:10.1007/978-3-030-15265-9_8

Muravchik, M., Gawthorpe, R. L., Sharp, I. R., Rarity, F., Hodgetts, D. 2018. Sedimentary environment evolution in a marine hangingwall dipslope setting. El Qaa Fault Block, Suez Rift, Egypt. Basin Research, 30, 452-478.

Nabawy, B. S., El Sharawy, M. S. 2015. Hydrocarbon potential, structural setting and depositional environments of Hammam Faraun Member of the Belayim Formation, Southern Gulf of Suez, Egypt. Journal of African Earth Sciences, 112, 93-110

Nabawy, B. S., Barakat, M. K. 2017. Formation evaluation using conventional and special core analyses: Belayim Formation as a case study, Gulf of Suez, Egypt. Arabian Journal of Geosciences, 10(2), 25

Naglaa, S., El-Kammar, A., 2013. Hydrocarbon Generating Basins and Migration Pathways in the Gulf of Suez, Egypt Life Science J 2013;10(5s):229-235] (ISSN:1097-8135).

Nguyen, C. D., Tran, X. V., Nguyen, K. X., Tran, H. N., Mai, T. T. 2019. The forming mechanisms of Oligocene combination/stratigraphic traps and their reservoir quality in southeast Cuu Long Basin offshore of Vietnam. Science and Technology Development Journal, 22(1), 185–195. doi:10.32508/stdj.v22i1.1216

Patton, T. L., Moustafa, A. R., Nelson, R. A., Abdine, S. A. 1994. Tectonic evolution and structural setting of the Suez Rift: Chapter 1: Part I. Type Basin: Gulf of Suez

Pivnik, D., M. Ramzy, B.L. Steer, J. Thorseth, Z. El Sisi, I. Gaafar, J.D. Garing, R.S. Tucker, 2003. Episodic growth of normal faults as recorded by syntectonic sediments, July oil field, Suez rift, Egypt, AAPG Bulletin, v. 87, p. 1015-1030.

Radwan, A.E., 2014. Petrophysical evaluation for Sidri and Baba members within Belayim Formation in the region of Badri field, Gulf of Suez, Egypt. M.Sc. Thesis DOI: 10.13140/RG.2.2.22772.09601

Radwan, A.E., 2018. New petrophysical approach and study of the pore pressure and formation damage in Badri, Morgan and Sidki fields, Gulf of Suez Region Egypt: PhD Thesis. DOI: 10.13140/RG.2.2.26651.82727

Radwan, A.E., 2020a. Modeling the Depositional Environment of the Sandstone Reservoir in the Middle Miocene Sidri Member, Badri Field, Gulf of Suez Basin, Egypt: Integration of Gamma-Ray Log Patterns and Petrographic Characteristics of Lithology. *Nat Resour Res*. https://doi.org/10.1007/s11053-020-09757-6

Radwan, A.E., 2020b. Wellbore stability analysis and pore pressure study in Badri field using limited data, Gulf of Suez, Egypt: AAPG/Datapages Search and Discovery Article #20476 (2020). DOI:10.1306/20476Radwan2020

Radwan, A.E., 2020c. Hydrocarbon Type Estimation Using the Synthetic Logs: A Case Study in Baba Member, Gulf of Suez, Egypt: AAPG/Datapages Search and Discovery Article #20475 (2020). DOI:10.1306/20475Radwan2020

Radwan, A.E., 2020d. Effect of Clay Minerals in Oil and Gas Formation Damage Problems and Production Decline: A Case Study, Gulf of Suez, Egypt: AAPG/Datapages Search and Discovery Article #20477 (2020). DOI:10.1306/20477Radwan2020

Radwan, A. E., Abudeif, A. M., Attia, M. M., Mahmoud, M. A. 2019a. Development of formation damage diagnosis workflow, application on Hammam Faraun reservoir: A case

study, Gulf of Suez, Egypt. Journal of African Earth Sciences, 153, 42–53. doi:10.1016/j.jafrearsci.2019.02.012

Radwan, A. E., Abudeif, A. M., Attia, M. M., Mohammed, M. A. 2019b. Pore and fracture pressure modeling using direct and indirect methods in Badri Field, Gulf of Suez, Egypt. Journal of African Earth Sciences, 156, 133–143. doi:10.1016/j.jafrearsci.2019.04.015

Radwan, A.E., Abudeif, A., Attia, M., MahmouD, M., 2019c. Formation Damage Diagnosis, Application on Hammam Faraun Reservoir: A Case Study, Gulf of Suez, Egypt. In: Offshore Mediterranean Conference. DOI: 10.13140/RG.2.2.22352.66569

Radwan, A.E., Abudeif, A., Attia, M., MahmouD, M., 2019d. Development of formation damage diagnosis workflow, application on Hammam Faraun reservoir: a case study, Gulf of Suez, Egypt. In: Offshore Mediterranean Conference. ISBN9788894043679-2019.

Radwan, A. E., Abudeif, A. M., Attia, M. M., Elkhawaga, M. A., Abdelghany, W. K., Kasem, A. A. 2020a. Geopressure evaluation using integrated basin modelling, well-logging and reservoir data analysis in the northern part of the Badri oil field, Gulf of Suez, Egypt. Journal of African Earth Sciences, 162, 103743. doi:10.1016/j.jafrearsci.2019.103743

Radwan, A. E., Kassem, A. A., & Kassem, A. 2020b. Radwany Formation: A new formation name for the Early-Middle Eocene carbonate sediments of the offshore October oil field, Gulf of Suez: Contribution to the Eocene sediments in Egypt. Marine and Petroleum Geology, 116, 104304. doi:10.1016/j.marpetgeo.2020.104304

Radwan, A. E., Abudeif, A. M., Attia, M. M. 2020c. Investigative petrophysical fingerprint technique using conventional and synthetic logs in siliciclastic reservoirs: A case study, Gulf of Suez basin, Egypt. Journal of African Earth Sciences, 167, 103868. doi:10.1016/j.jafrearsci.2020.103868

Radwan, A. E., Trippetta, F., Kassem, A. A., Kania, M. 2020d. Multi-scale characterization of unconventional tight carbonate reservoir: Insights from October oil filed, Gulf of Suez rift

basin, Egypt. Journal of Petroleum Science and Engineering, 107968. doi:10.1016/j.petrol.2020.107968

Radwan, A.E., Nabawy, B.S., Kassem, A.A. *et al.* 2021. Implementation of Rock Typing on Waterflooding Process During Secondary Recovery in Oil Reservoirs: A Case Study, El Morgan Oil Field, Gulf of Suez, Egypt. *Nat Resour Res.* https://doi.org/10.1007/s11053-020-09806-0

Radwan, A., Sen, S., 2020. Stress Path Analysis for Characterization of In Situ Stress State and Effect of Reservoir Depletion on Present-Day Stress Magnitudes: Reservoir Geomechanical Modeling in the Gulf of Suez Rift Basin, Egypt. Nat Resour Res. https://doi.org/10.1007/s11053-020-09731-2

Rohais, S., Barrois, A., Colletta, B., Moretti, I. 2016. Pre-salt to salt stratigraphic architecture in a rift basin: insights from a basin-scale study of the Gulf of Suez (Egypt). Arabian Journal of Geosciences, 9(4), 317.

Rohais, S., Rouby, D. 2020. Source-to-Sink Analysis of the Plio-Pleistocene Deposits in the Suez Rift (Egypt). In Arabian Plate and Surroundings: Geology, Sedimentary Basins and Georesources (pp. 115-133). Springer, Cham.

Rashed, A. 1990. The main fault trends in the Gulf of Suez and their role in oil entrapment. In 10th Petroleum exploration and production Conference, Cairo, November, Part I (pp. 43-178).

Richardson, M., Arthur, M. A. 1988. The Gulf of Suez—northern Red Sea neogene rift: a quantitive basin analysis. Marine and Petroleum Geology, 5(3), 247-270

Rohrback, B. G. 1982. Crude oil geochemistry of the Gulf of Suez: Egyptian General Petroleum Corporation. In 6th International Exploration Conference, Cairo

Salah, M. G., Alsharhan, A. S. 1997. The Miocene Kareem Formation in the southern Gulf of Suez, Egypt: a review of stratigraphy and petroleum geology. Journal of Petroleum Geology, 20(3), 327-346

Salama, A., El-Mougy, S., El-Moniem, M.A., Hakim, S., 1994. Exploration in the southern Gulf of Suez area, Egypt, vol. 1. In: 10th Egyptian General Petroleum Exploration, Petroleum Exploration and Production Conference, pp. 104–143.

Sarhan, M. A. 2020. Geophysical appraisal and oil potential for Rudeis Formation at West Hurghada area, southern Gulf of Suez: detection of stratigraphic trap. Arabian Journal of Geosciences, 13(6), 1-9.

Schlumberger. 1989. Log interpretation principles/applications manual.

Schlumberger Well Services. 1986. Log interpretation charts. Schlumberger Well Services.

Serra, O. E. 1983. Fundamentals of well-log interpretation.

Shaheen, A. N., Shehab, M. 1984. Petroleum generation, migration and occurrence in the Gulf of Suez offshore, south Sinai: 7th Egyptian General Petroleum Corporation. In Petroleum Exploration and Production Conference (Vol. 1, pp. 126-152).

Shepherd, M., 2009. Volumetrics, in M. Shepherd, Oil field production geology: AAPG Memoir 91, p. 189–193.

Sladen, C., Chiarella, D. 2020. Lake systems and their economic importance. Regional Geology and Tectonics: Principles of Geologic Analysis, 313–342. doi:10.1016/b978-0-444-64134-2.00034-1

Stirling, E. J., Fugelli, E. M. G., Thompson, M. 2017. The edges of the wedges: a systematic approach to trap definition and risking for stratigraphic, combination and sub-unconformity traps. Geological Society, London, Petroleum Geology Conference Series, 8(1), 273–286. doi:10.1144/pgc8.19

Tawadros, E., 2012. History of Geology in Egypt. Earth Sciences History, 31(1), 50–75. doi:10.17704/eshi.31.1.h8273w68185p7q7g

Tewfik, N., Harwood, C., Deighton, I., 1992. The Miocene, Rudeis and Kareem Formations in the Gulf of Suez: Aspects of sedimentology and geohistory. 11th EGPC. Exploration Seminar, Cairo, 1, 84–113.

Ungerer, P., Chénet, P. Y., Moretti, I., Chiarelli, A., Oudin, J. L. 1986. Modelling oil formation and migration in the southern part of the Suez rift, Egypt. Organic Geochemistry, 10(1-3), 247-260

Wescott, W.A., Krebs, W.N., Dolson, J.C., Karamat, S.A. Nummedal, D.1996. Rift basin sequence stratigraphy: some examples from the Gulf of Suez. GeoArabia, 1, 343-357.

Wever, H. E. 2000. Petroleum and source rock characterization based on C7 star plot results: Examples from Egypt. AAPG bulletin, 84(7), 1041-1054

Wyllie, M. R. J., Rose, W. D. 1950. Some theoretical considerations related to the quantitative evaluation of the physical characteristics of reservoir rock from electrical log data. Journal of Petroleum Technology, 2(04), 105-118.

Young, M. J., Gawthorpe, R. L., Sharp, I. R. 2000. Sedimentology and sequence stratigraphy of a transfer zone coarse-grained delta, Miocene Suez Rift, Egypt. Sedimentology, 47(6), 1081–1104. doi:10.1046/j.1365-3091.2000.00342.x

Young, M. J., Gawthorpe, R. L., Sharp, I. R. 2003. Normal fault growth and early syn-rift sedimentology and sequence stratigraphy: Thal Fault, Suez Rift, Egypt. Basin Research, 15(4), 479–502. doi:10.1046/j.1365-2117.2003.00216.x

Youssef, A. 2011. Early–Middle Miocene Suez syn-rift-basin, Egypt: a sequence stratigraphy framework. GeoArabia, 16(1), 113-134.

Caption of Figures

Fig. 1 A) Structural map of the Suez rift (after Rohais et al., 2016 and references herein). Hatched areas indicate major accommodation zones. Position of the Badri field and distribution of major oil field are highlighted in green (modified from Alsharhan, 2003). Red line indicate the cross sections presented in Figure 2. B) Geodynamic setting of the Gulf of Suez (red box). Major elements of the Aqaba–Levant intra-continental transform boundary, the Bitlis-Zagros convergence zone and the Red Sea – Gulf of Aden are highlighted. C) Simplified stratigraphic column of the Suez rift (after Rohais et al., 2016 and references herein).

Fig. 2 Southwest-northeast cross-section through the Suez Rift Basin (after EGPC, 1996). See figure 1A for the line of section position.

Fig. 3 Structure contour map of Baba Member in the Badri field. Position of the studied wells (A – D) is also indicated. X and y coordinates are related to the projection coordinates of Egypt Gulf of Suez S-650 TL/Red Belt.

Fig. 4 Stratigraphic scheme of Gulf of Suez for the Miocene to Pliocene interval (modified after Wescott et al., 1996; Bowsorth and McClay, 2001). Sea-level is derived from Haq and Al-Qahtani (2005). Stratigraphy and ages are from Hardenbol et al. (1998), and Gradstein et al., (2012), respectively.

Fig. 5 A) Standard composite lithology log of the Belayim Formation used in the Badri Field versus B) the composite lithology log derived from the studied Badri (A, B, C and D) wells.

Fig. 6 Stratigraphic correlation of Baba sandstones facies through Badri (A, B, C and D) wells.

Fig. 7 Paleo-lithological maps for the Belayim Formation (Baba, B4) in the vicinity of the Morgan Accommodation Zone (modified from Rohais et al., 2016). A. Map with dominant lithology for the basal evaporite deposits recorded in the Badri field. B. Map with dominant lithology for the Shale/Sandstones clastic interval interbedded in Baba evaporite. Sandstones are preserved in the northern part of the Badri field.

Fig. 8 QFL triangular diagram showing the classification of Baba sandstones reservoir.

Fig. 9 Microphotographs from the A well. (A) Sub-rounded quartz grains with intergranular porosity; magnifications 80X, Sample depth of 2060 m. (B) Intragranular porosity formed due to leaching of feldspars, magnifications 80X, crossed nicols. Sample depth of 2060 m. (C) Sandstones with plagioclase (highly lamellar twinning), anhydrite cement; magnifications 80X. Sample depth of 2066 m. (D) Organic material filling pore space. magnifications 80X, crossed nicols. Sample depth of 2066 m.

Fig. 10 Microphotograph from the D well. (A) Anhydrite cement between quartz grains; magnifications 80X. Sample depth of 2069 m. (B) Feldspars within a composite grain showing polycrystalline quartz indicating a metamorphic source (gneiss); magnifications 80X, crossed nicols. Sample depth of 2080 m. (C) Arkosic sandstones with lamellar twinning of plagioclase, magnifications 80X. Sample depth of 2080 m. (D) Porosity around grains under crossed nicols. magnifications 80X. Sample depth of 2075 m.

Fig. 11 A) Computer processed interpretation (CPI) for the well B where, GR is Gamma-ray curve, RHOB is the Bulk Density curve, NPHI is the neutron porosity, RT is resistivity, EFF-Porosity is the effective porosity, SW_AR is the water saturation using Archie equation. The last column indicates the lithology content where yellow is the quartz, grey is the shale content, pink is the feldspar, plum is the anhydrite and green is the oil saturation (white with red circle indicates the gas saturation). **B)** The computer processed interpretation (CPI) for the well C.

Fig. 12 Cross section through the Badri (A, B, C and D) Wells, (refer to Figure 3 for the line of section position).

Fig. 13 Events chart for the Badri Field. Formations abbreviations: NEZ = Nezzazat, N = Nukhul, R = Rudeis, K = Kareem, B = Belayim, SG = South Gharib and Z = Zeit.

CRediT author statement

Ahmed Radwan: Lead, Conceptualization, Methodology, Software, Investigation, Writing-Original draft preparation, Reviewing and Editing, **Sébastien Rohais.**: Reviewing and Editing, Software. **Domenico Chiarella:** Reviewing and Editing.

Declaration of interests

☒ The authors declare that they have no known competing financial interests or personal relationships that could have appeared to influence the work reported in this paper.

☐The authors declare the following financial interests/personal relationships which may be considered as potential competing interests:

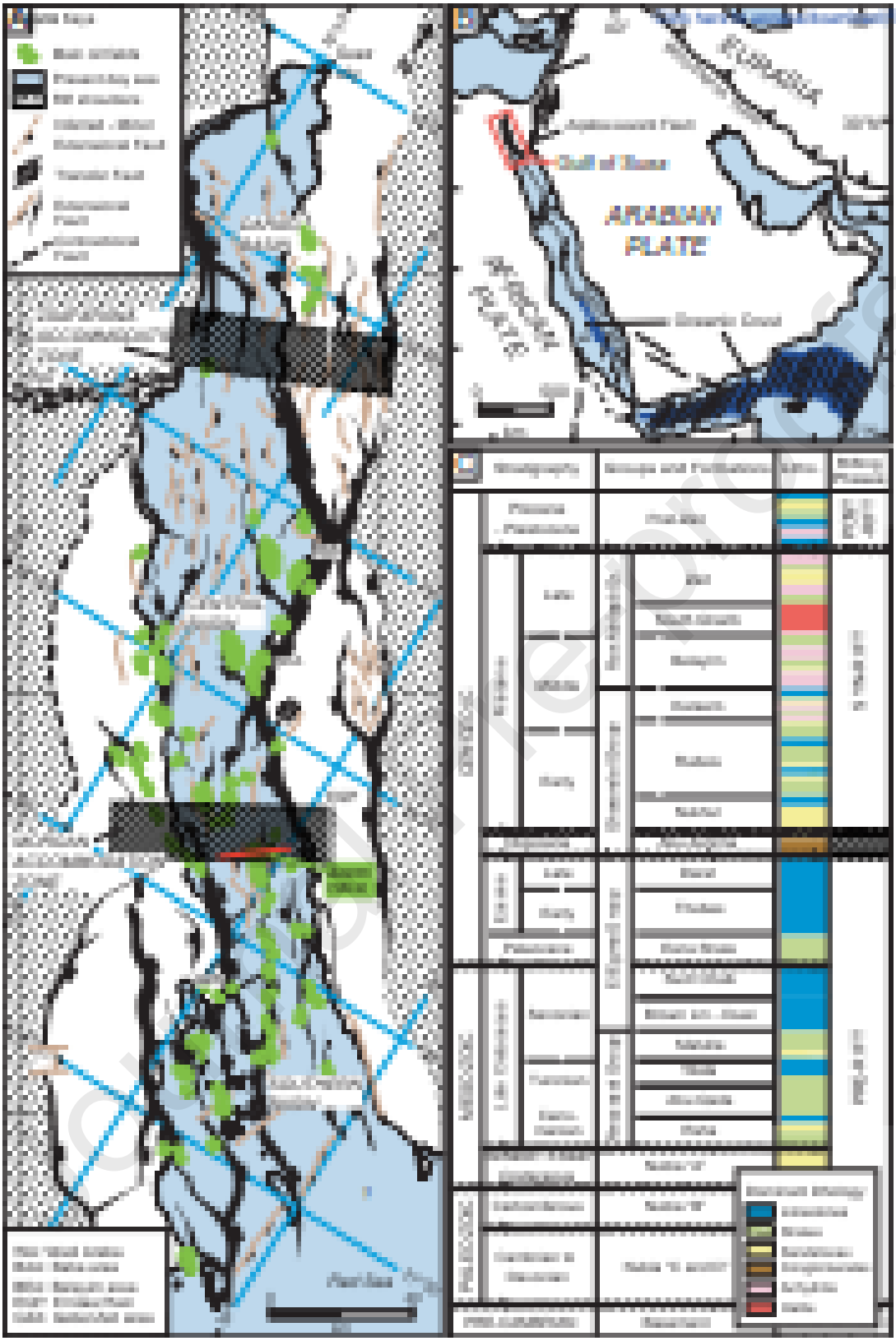
ARABIAN
PLATE

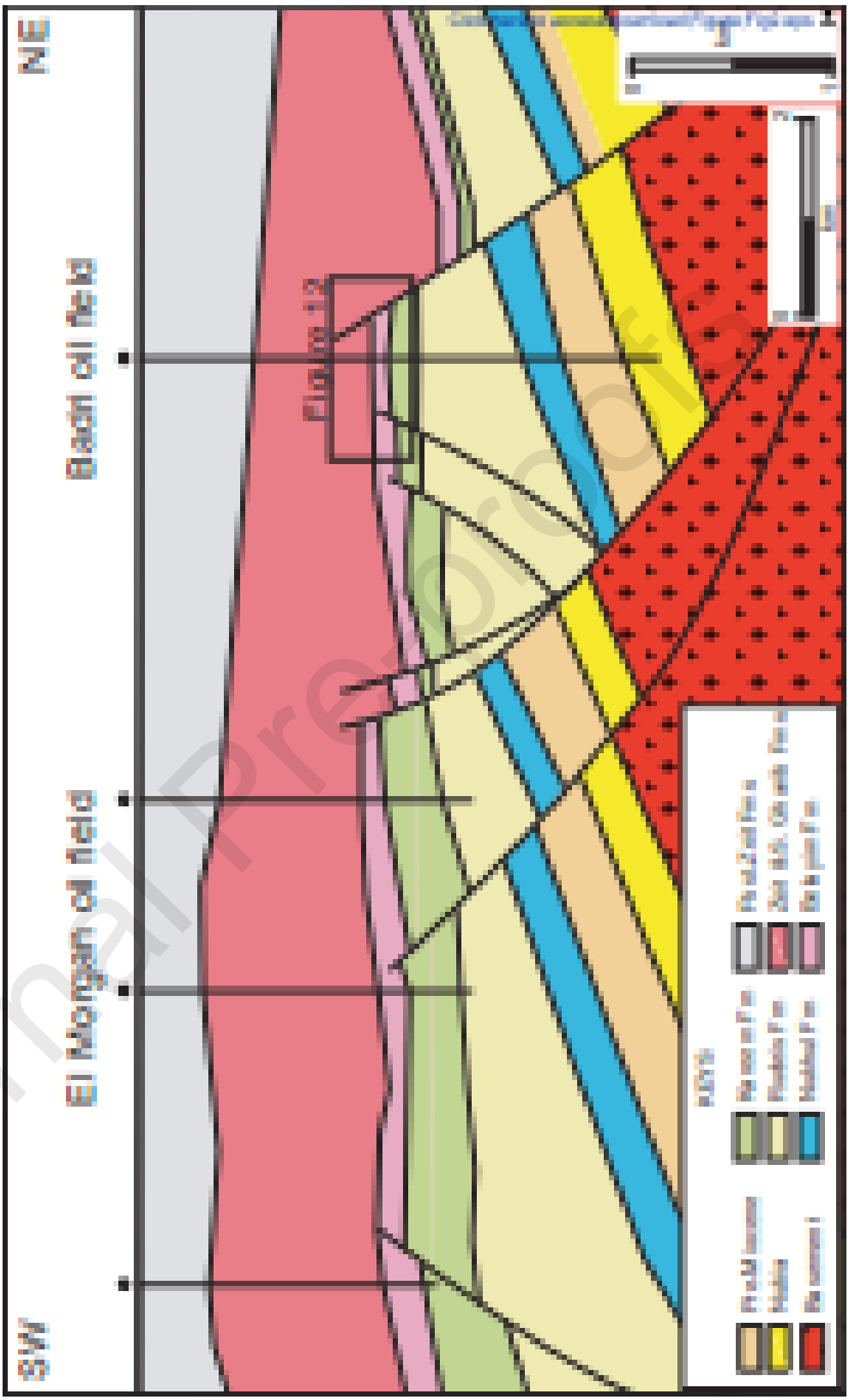

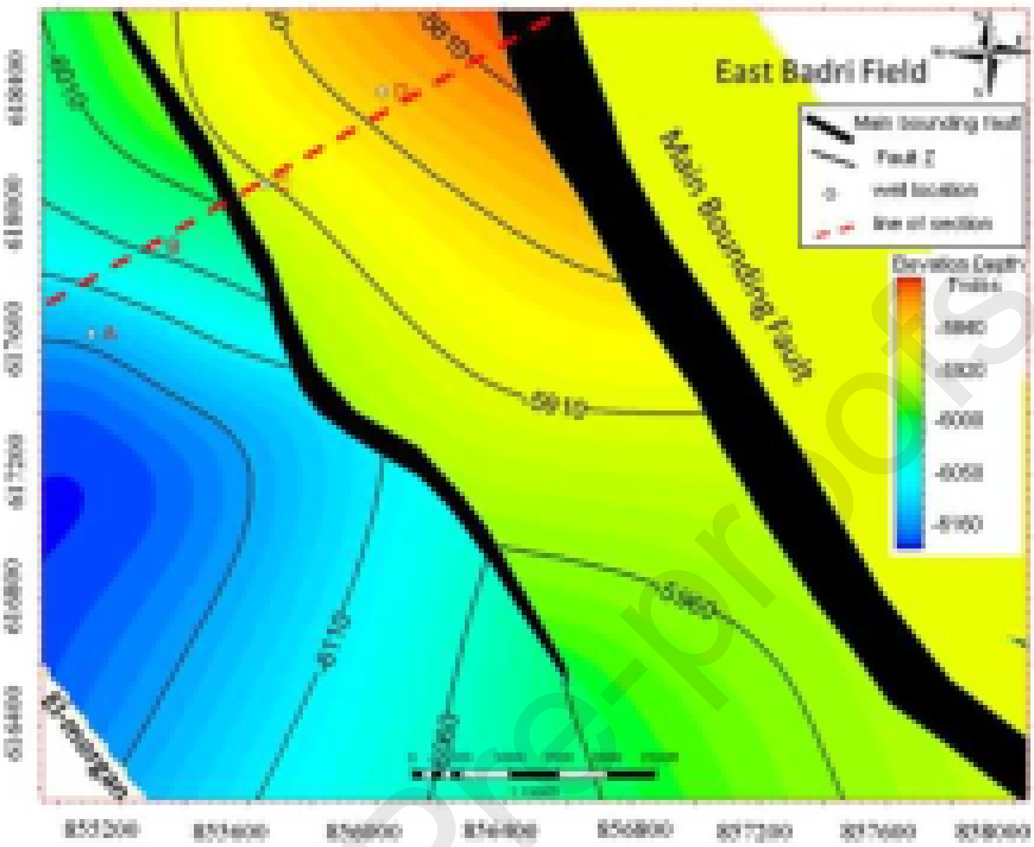
East Badri Field
Main Bounding Fault
well location
line of section
855200
855600
856000
856400
856800
857200
857600
858000

Figures

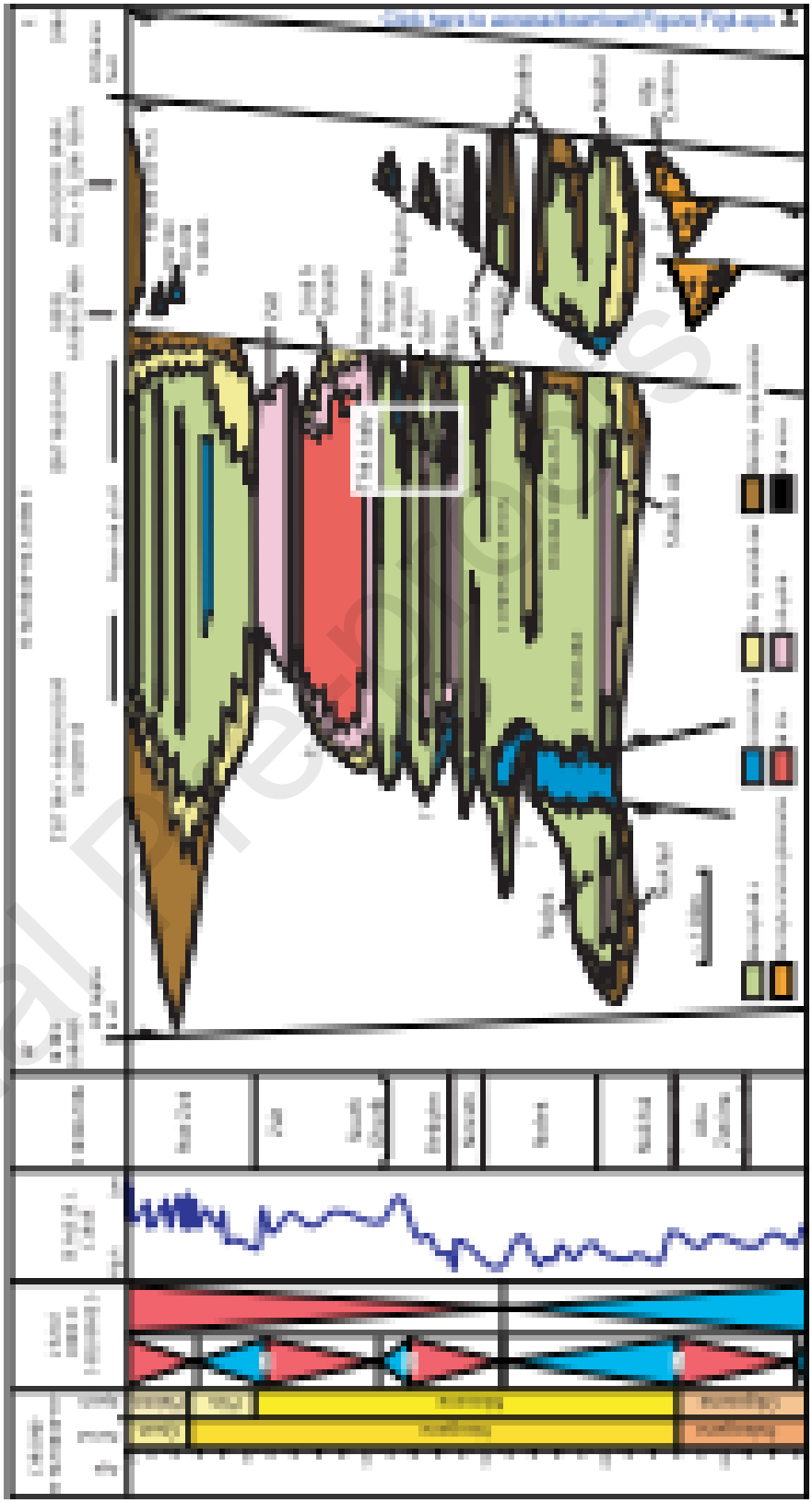

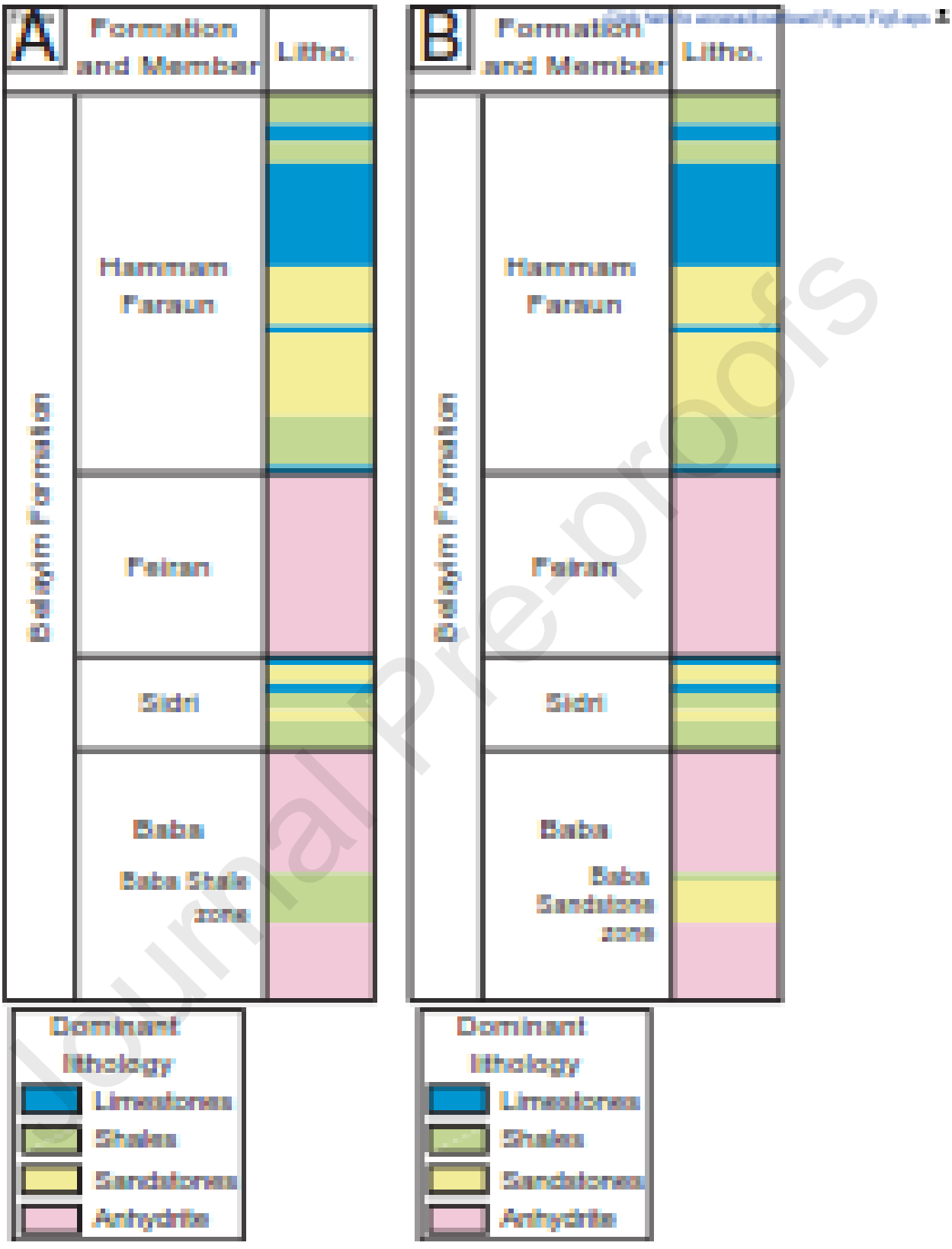

Figure

Click here to access/download/Figure/Fig6.JPG

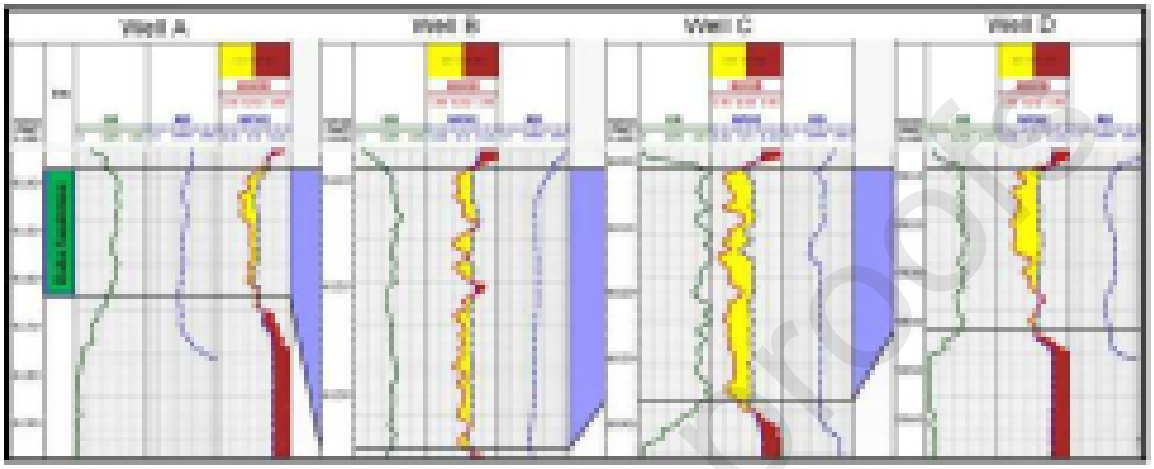

Figure

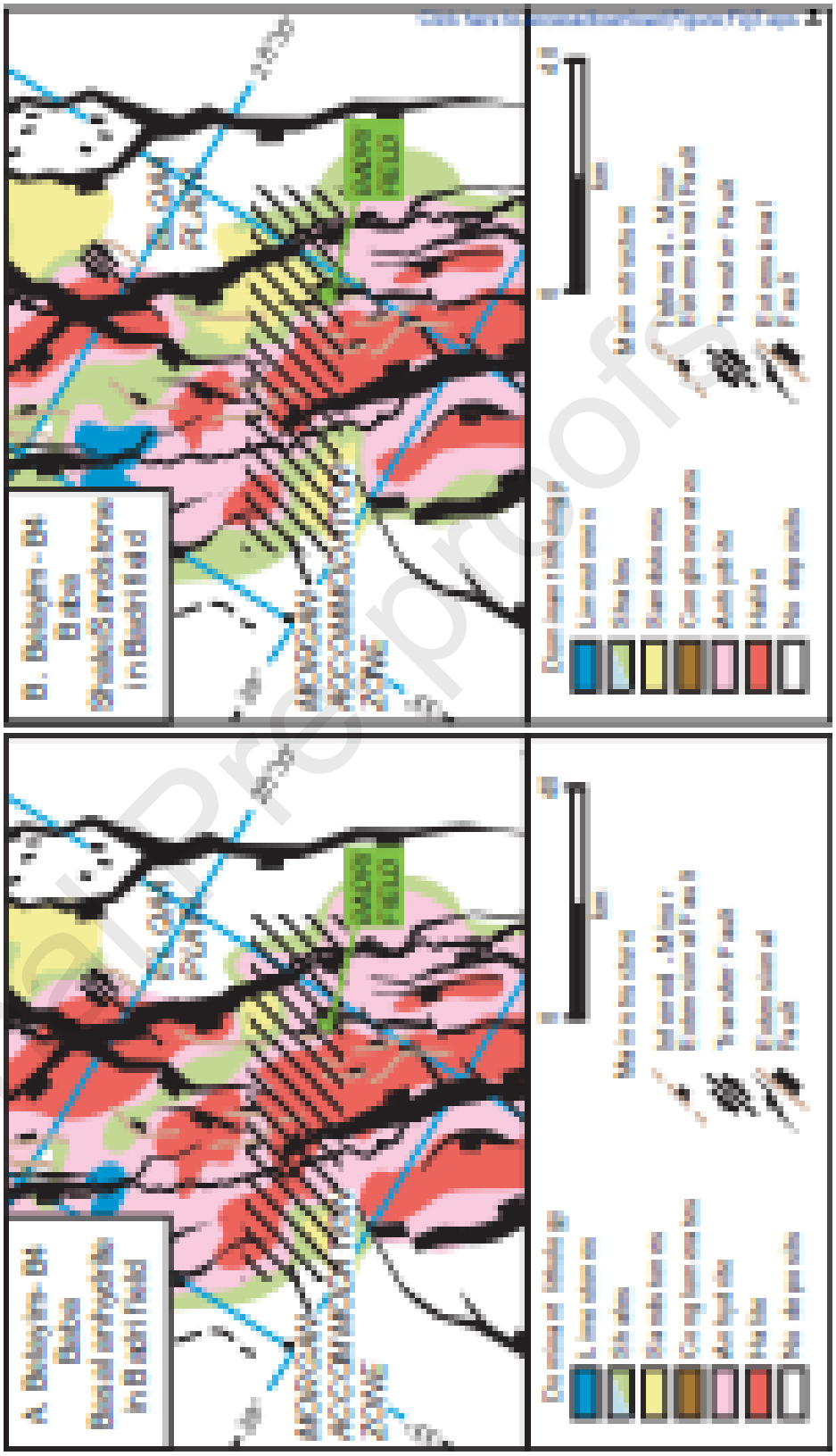

Figure

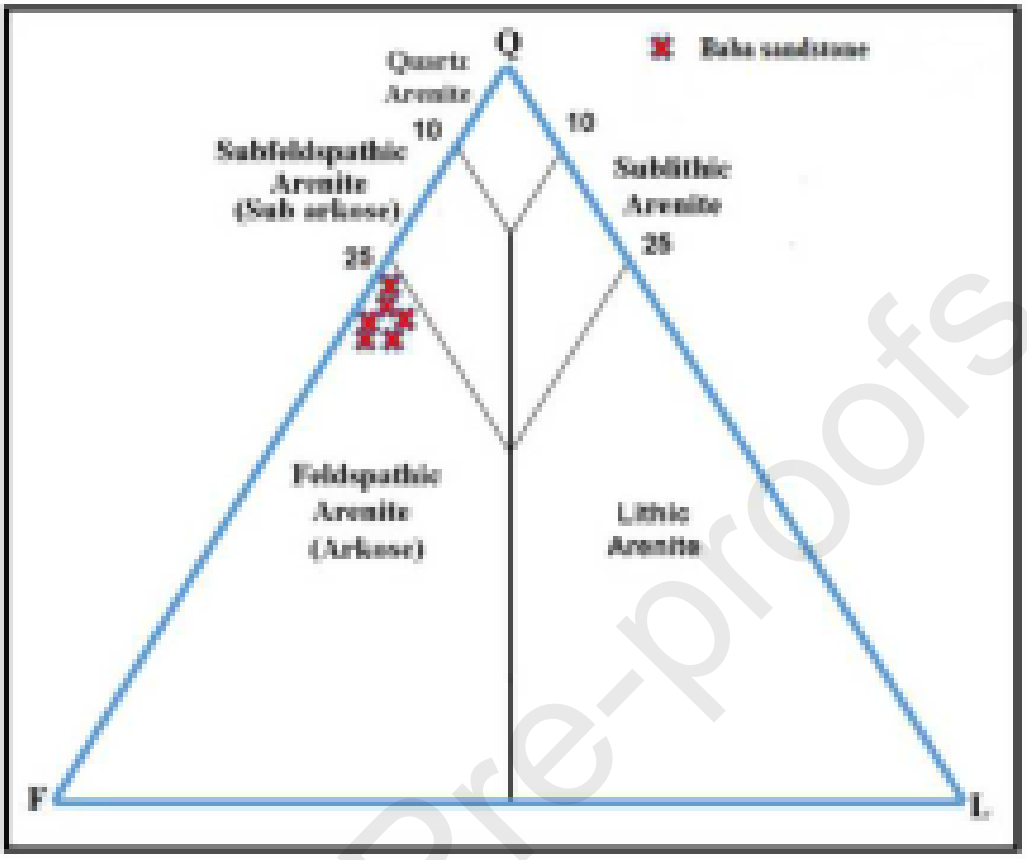

Figure

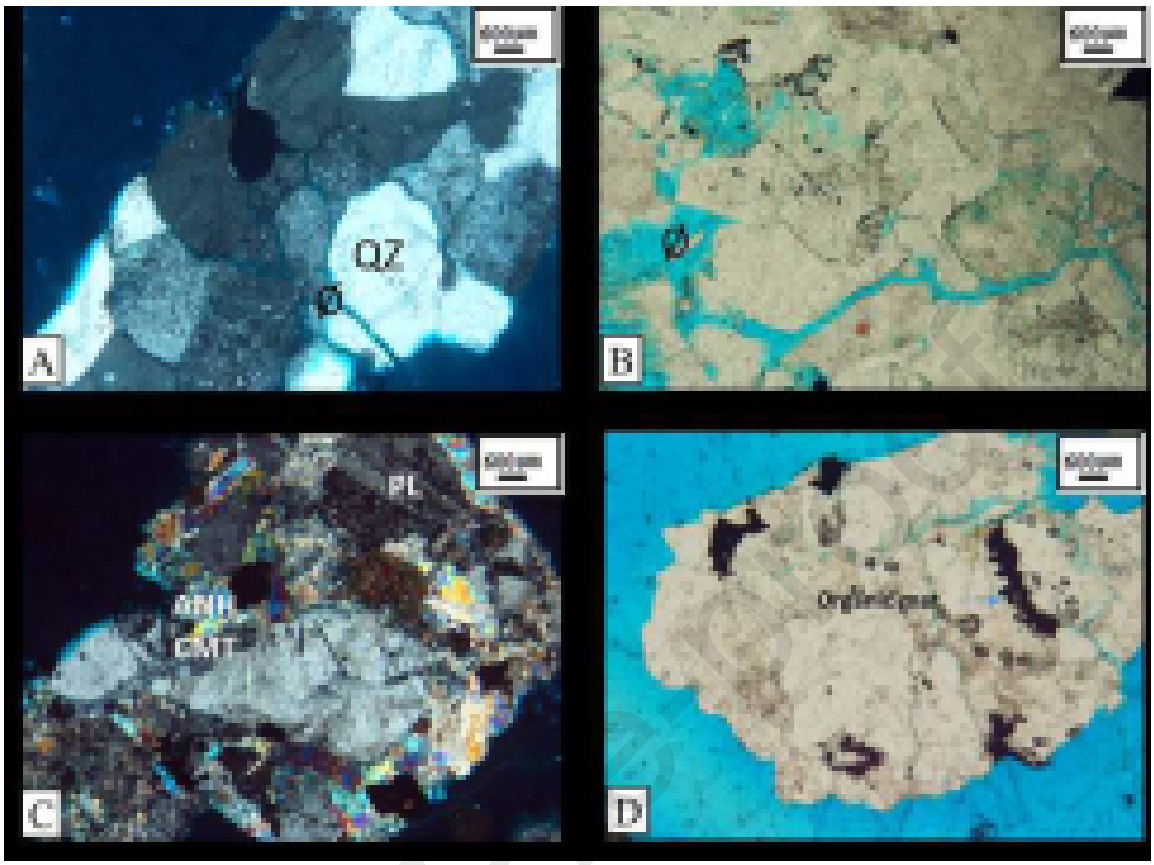

Figure

Click here to access/download Figure Fig1 1.jpg

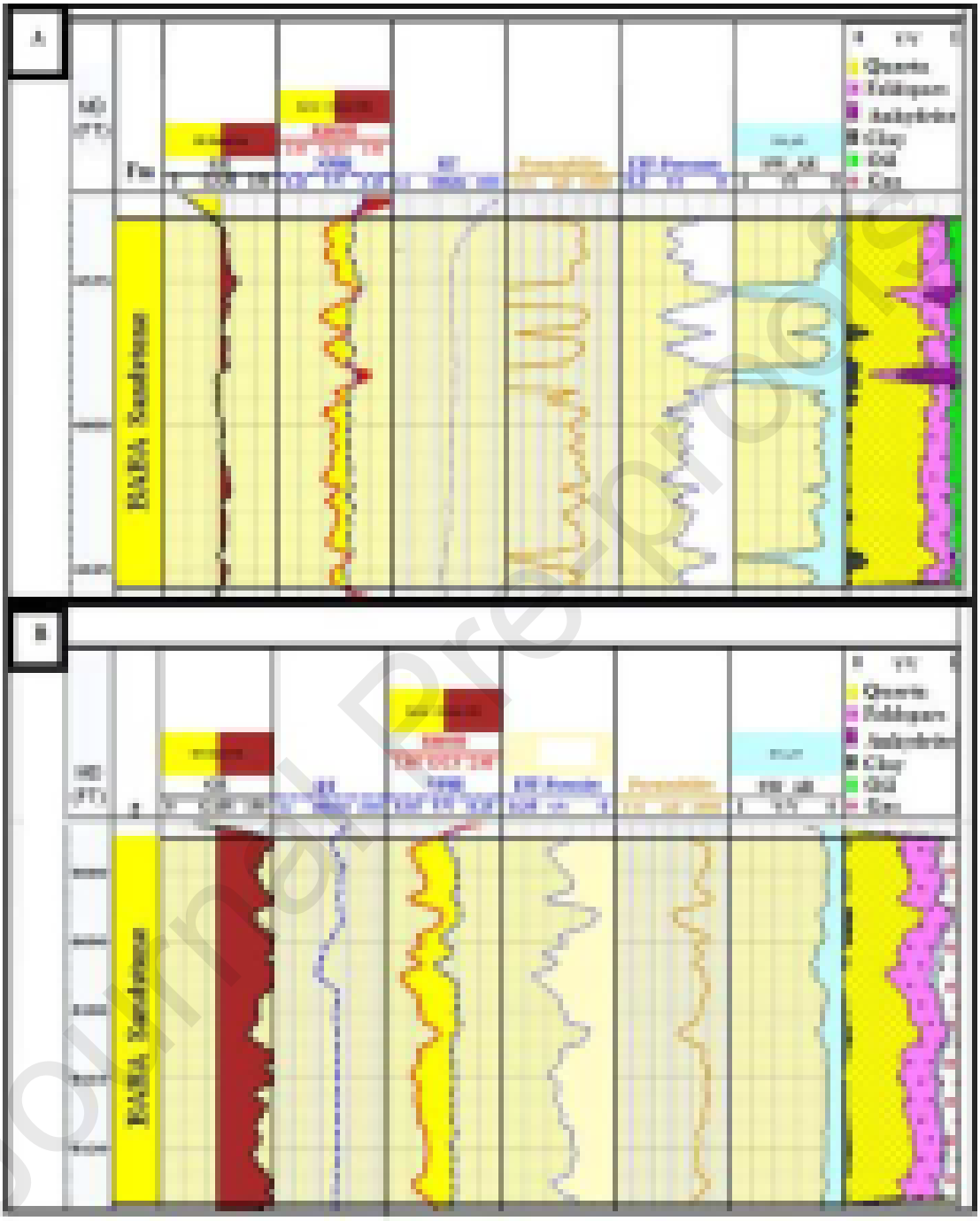

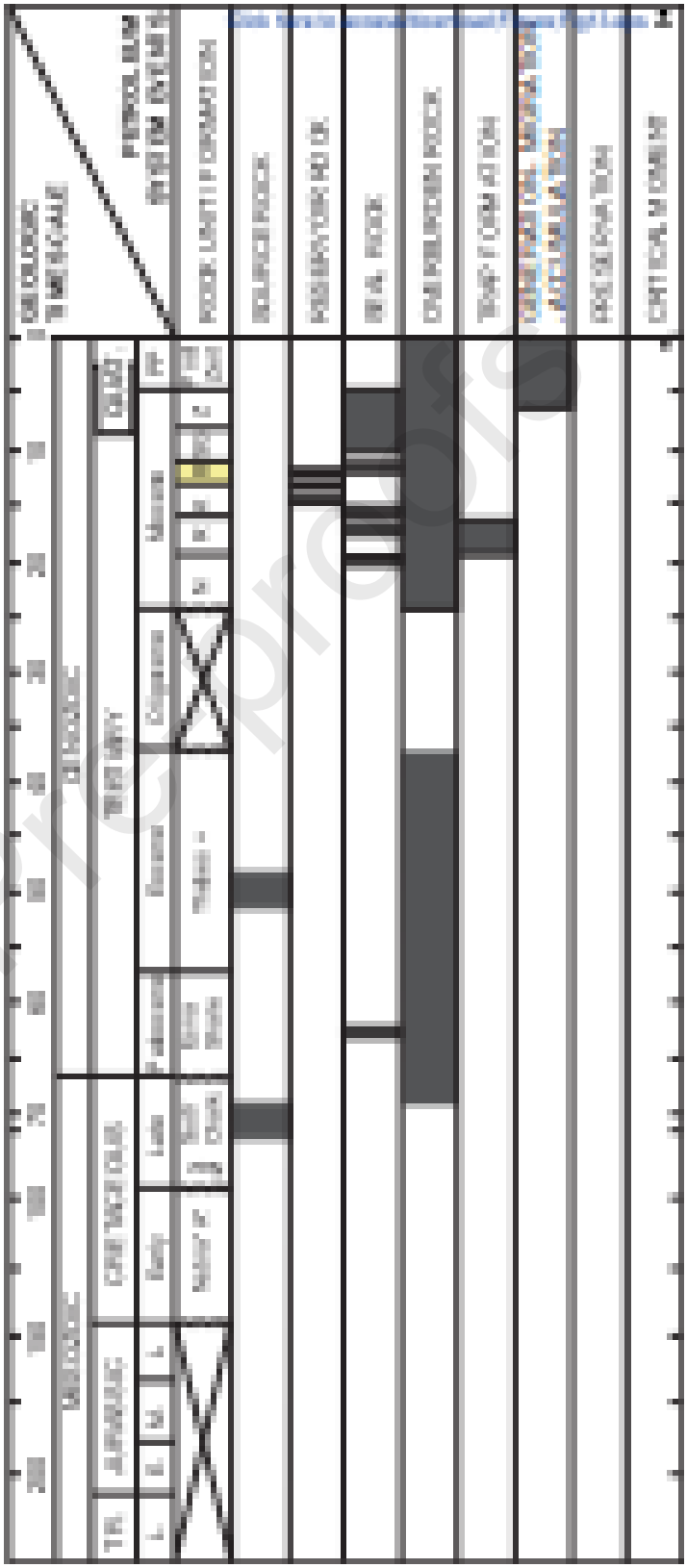

Table 1 List of the used standard equations in the petrophysical evaluation.

Equation	Equation number	Expressions
Vsh = ΦN- ΦD / ΦNsh- ΦDsh	1	ØN= neutron porosity in sand, ØD= density porosity in sand, ØNsh= neutron porosity adjacent shale, ØDsh= density porosity in adjacent shale.
$\Phi t = \sqrt{\Phi N2- \Phi D2/2}$	2	(Φ t) = Total porosity from neutron or any method (fractional)
Φeff = Φt −Vcly *Φsh)	3	(Φ eff) = Effective porosity (fractional), (Vcly) =Volume of clay from non-linear equation or any (fractional), (Φ sh) =Neutron porosity reading in 100% shale.
$Sw = n\sqrt{a.Rw/\Phi m.Rt}$	4	Rt is the deep resistivity, Rw is the down hole water resistivity, Sw is the water saturation, a is the Archie's exponent, m is the cementation factor, n is the saturation exponent,
K=(250*Φ3 / Swir)2 medium gravity oil	5	K is the permeability in millidarcy, Φ is the porosity; Swir is the irreducible water saturation.
K=(79*Φ3 / Swir)2 dry gas	6	
STOOIP = 7758 AhØ(SO) / BO (STB)	7	STOOIP= stock-tank original oil in place [barrels], G= gas initially in place [MM SCF], A= Area [acres], h = Net pay thickness [feet], 7758 = Conversion factor (acre-ft * 7758 = barrels), Ø = Porosity of this net reservoir rock (decimal), So= Oil saturation - oil-filled portion of this porosity (decimal), Bo = Formation Volume Factor for oil (decimal)
GIIP =43,560 AhØ(Sg) / Bg (MM SCF)	8	(Bg) = Formation Volume Factor for gas (decimal)

Table 2 Summary of the average petrophysical characteristics for Baba Sandstone in the studied wells.

well	A	B	C	D
Thickness (ft)	28	20	36	38
Vsh (%)	12	13	11	9
PHIE (%)	16	12	17	18
Sw (%)	17	21	12	14
Shr (%)	83	79	88	86
K (mD)	180	183	220	200
Gross (ft)	28	20	36	38
Pay(ft)	28	20	36	38
NGR	1	1	1	1

Table 3 Visual estimates of whole-rock composition for the studied zone samples. Sorting: W= Well; M= Moderate; P= Poor. Roundness: R= Rounded; SR= sub-rounded; SA= sub-angular. Grain size is in microns. Values in ( ) represent % not included in total percent.

Sample	Constituent grains (%)				Cement/Matrix (%)					Text/ Fabric			Porosity (%)		
number	Quartz	Feldspar	Lithics	accessory	calcite	silica	Anhydite	clay	organics	Average grain size	sorting	rounding	Total	primary	secondary
1	67	27	2	1		(1)	1	1	1	400	M	SR	14	12	2
2	72	25	1					2	2	340	M	SR	15	14	1
3	70	25	3	2		(1)	2	1	1	460	M/W	SR	13	11	2
4	69	26	1				2	2		380	M/P	SA	14	12	2
5	70	25	1	1		(2)	1	2		160	P/M	SR	12	11	1
6	65	30	2	1				2		280	M	SA	11	9	2
7	66	28	1	1		(2)	1	1		290	P	SA	15	13	2
8	72	26						1	1	330	M	SR	13	11	2
9	70	27		1				1	1	480	W	SA	14	13	1
10	69	29		1				1		500	W	SR	14	13	1
11	73	25		1					1	470	W	SR	13	11	2
12	67	31	1					1		450	M	SA	15	14	1
13	69	27	2	1			1			380	W	SR	12	10	2
14	70	24	1	2		(1)	2			520	M	SR	15	14	1
15	66	27	1	1		(3)	1	2	1	490	M/W	SR	15	13	2
16	72	26				(1)	1		1	600	M	SA	14	13	1
17	71	24		1		(2)	1	1	1	560	W	SA	13	11	2
18	68	27	1	2		(3)	1	1	1	440	M/P	SR	14	12	2
19	69	28	1			(2)	1		1	420	P	SR	14	13	1
20	72	26		1		(2)		1		390	M	SR	15	13	2
21	74	25		1		(2)				520	M	SR	15	14	1
22	70	26	1	1		(3)		1	1	510	W	SA	15	13	2
23	71	27				(1)	1		1	490	W	SR	13	11	2
24	69	27	1			(2)	1	1	1	470	M/W	SA	12	10	2
25	68	28	1			(2)	1	1	1	390	M	SR	14	12	2
26	72	26		1		(3)			1	280	M/P	SR	14	12	2
27	70	28		1		(2)	1			290	M/W	SR	15	13	2
28	69	29		1		(2)		1		330	M	SR	15	13	2
29	68	30	1			(2)	1			510	W	SR	11	10	1
30	71	28				(2)		1		480	M	SR	13	11	2

Table 4 Summary of the Source rock parameters for the Badri field, where TOC, total organic carbon; S_2, hydrocarbons from kerogen cracking; S_3, organic CO_2—kerogen derived; T_{max}, pyrolysis temperature at which maximum emission of hydrocarbons occurs, R_o, Vitrinite reflectance.

Source rock parameters		
Formation and age	Brown Limestone (Senonian); Thebes Formation (Eocene)	Unit
Lithology	Limestone	
Depositional system	Open marine	
TOC	4% (2-8% regionally)	%
Kerogen type	II and II/I	
Time of hydrocarbon expulsion	Late Miocene to Pliocene	
Hydrogen index (HI)	300–675 average (450)	mg HC/gm of TOC
Oxygen index (OI)	15-100 average (54)	mg HC/ gm of CO_2
S2	19.58	mg HC/gm rock
Tmax (°C)	422	(°C)
Ro	0.7	%
Time of hydrocarbon expulsion	Late Miocene to Pliocene	
API gravity	Belayim: 27°; Kareem: 28°	°API

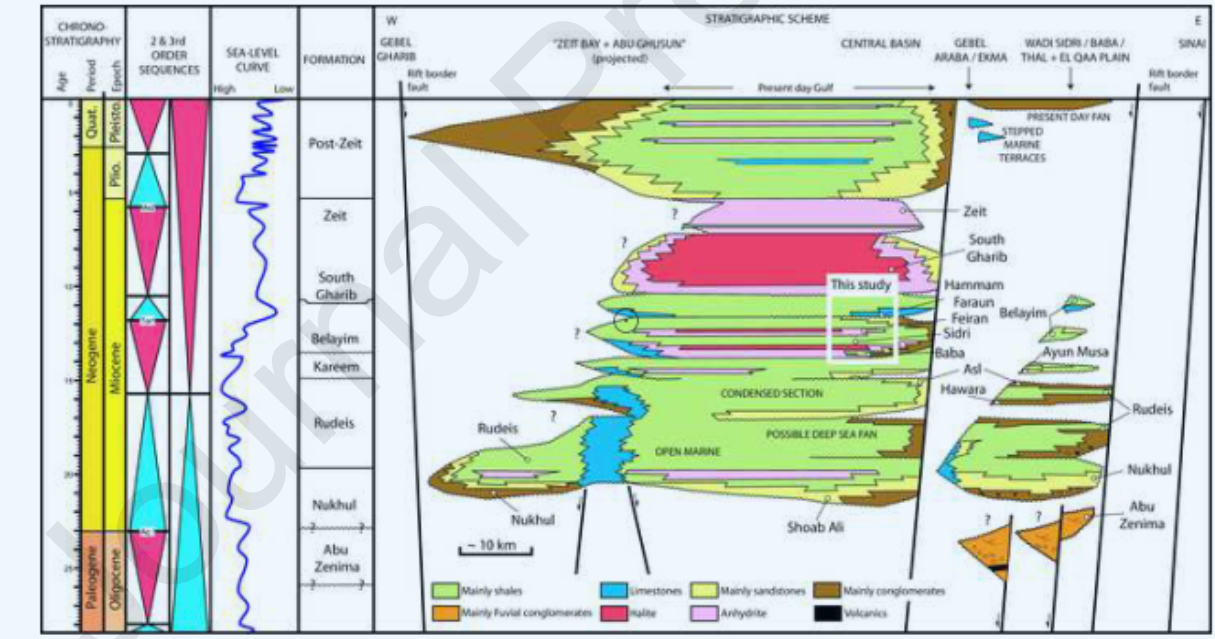

Highlights

- Combined stratigraphic-structural trap potentiality
- Multi dataset as successful exploration approach
- Gulf of Suez exploration potentiality
- Hydrocarbon potentiality in the middle Miocene Baba sandstones